Calculation of Raman scattering by acoustic phonons in superlattices

O. Pilla* and V. Lemos

*Instituto de Física "Gleb Wataghin," Universidade Estadual de Campinas (UNICAMP),
13083-970 Campinas, São Paulo, Brazil*

M. Montagna

Dipartimento di Fisica, Università degli Studi di Trento, I-38050 Povo, Trento, Italy
(Received 23 May 1994)

We report on the calculation of low-frequency Raman scattering by longitudinal acoustic phonons in superlattices. The phonons are treated as elastic waves propagating in a continuum and their mode patterns are calculated by a transfer-matrix method. The electromagnetic propagation is calculated neglecting reflections and refractions at the interfaces, through the use of the same index of refraction for both constituent materials. The use of a complex refraction index allows for absorption effects to be included. The suitability of the numerical calculation for modeling superlattices is demonstrated.

I. INTRODUCTION

Raman scattering by folded phonons in semiconductor superlattices (SL's) has been successfully analyzed with the help of dispersion relations.[1-3] Even though peak positions fit very well in the dispersion curves a detailed description of the spectra is still missing. Apart from the folded phonon studies, additional features arising from resonance processes,[2] and secondary oscillations observed in the spectra,[4] require quantitative interpretation. Several theoretical approaches propose analytical expressions for the relative intensities of the acoustic modes.[5-7] Among those treatments, one of the most complete includes, besides the elastic wave propagation, photoelastic and electromagnetic modulation.[6] However, the experimental profiles, and, in particular, the relative intensities of the lines have not been reproduced.[8] Actually, the spectra cannot be described in detail because of the oversimplifying assumption of infinite superlattice to account for the periodicity of the wave functions in the SL. The need for modeling a finite structure was pointed out previously for several different microstructures.[4,9,10] The model employed by the authors[4,9,10] was based on a linear chain dynamic. Their calculation consists of diagonalization of the dynamical matrix of high dimensionality, equal to the total number of atomic layers in the structure. This includes the SL, the capping layer and a finite number of atomic layers of the substrate, resulting in a long computational procedure. Besides that, comparison with experiment required convolution with a Lorentzian line shape with a broadening factor, Γ, as an adjustable parameter, which is just phenomenological. An alternative approach was accomplished through the calculation of elastic response of a series of multilayered finite-size structures in terms of the elastic properties of their constituents.[11] The wave equation in each layer was solved with appropriate boundary conditions at each interface by using the matrix-transfer method. A most interesting aspect explored in Refs. 11 is the possibility of selectively transmitting or reflecting phonons in

some frequency range leading to the perspective of application to phonon devices. The analytical expression for the transmission rate thus derived was not exceedingly complicated because the treatment was restricted to just the elastic propagation through simple microstructures. If a more complex microstructure is to be handled, or if the constituent materials have lower symmetry, then numerical methods are required.

Here, we propose a numerical calculation to improve the solution of light scattering by longitudinal acoustic phonons in finite superlattices. The phonons are treated as elastic waves of a continuum and their propagation is defined by the transfer-matrix method.[6,11] Our method takes into account the absorption of the light through the imaginary part of the refraction index. This is very important in order to describe the line shapes not only for highly absorbing materials but also for lesser absorbing ones, and even far from the Bragg light reflection condition, in contrast to previous conclusions.[12] The acousto-optic parameters of the materials are taken as free parameters to fit the relative intensities of the Raman lines. The model accounts for all features of the spectra, including weak oscillations related to the finite number of periods. The output gives values for physical constants that can be discussed in the light of well known values for bulk materials.

II. GENERAL CONSIDERATIONS

We consider at first an homogeneous medium under an incident wave of the type $\overline{E} = \overline{E_0} e^{i\overline{k}_{\text{in}}\overline{r}}$, where $\overline{k}_{\text{in}}$ is the wave vector of the light. In a backscattering geometry, only the longitudinal acoustic phonons propagating along the z axis contribute to the scattering, and all the information of the Brillouin spectrum is contained in the following expression:[5]

$$I_{xx}(\omega_p) \propto \left| \int_V e^{-iqz} \frac{\partial u_z(p,z)}{\partial z} P_{xxyy}(z) dz \right|^2 \qquad (1)$$

where $q = k_{out} - k_{in} \approx -2k_{in} = -2nk_0$, n is the refraction index, and k_0 is related to the light wavelength in vacuum λ_0 by $k_0 = \frac{2\pi}{\lambda_0}$. P is the photoelastic tensor, and $u(p,z)$ are the normalized displacements from the equilibrium positions of the medium at the position z, under the normal mode of vibration of index p and energy ω_p. The integration is performed on the scattering volume V. Equation (1) is a low-frequency, high temperature approximation, when $\rho(\omega)N(\omega,T)/\omega \propto T$ since the density of states $\rho(\omega) \propto \omega^2$ and the Bose factor $N(\omega,T) \propto kT/\hbar\omega$.

A SL, consisting of alternating layers of two different cubic crystal with [001] direction along the SL axis z, is a more complicated system. Here, the electric field $\overline{E}$ is no longer a sinusoidal wave because several refractions and reflections take place at the interfaces between layers.

Considering a backscattering geometry along the z direction from a SL with perfectly sharp interfaces, the following relation for the electromagnetic field inside the superlattice holds:

$$\begin{pmatrix} E(z + \Delta z) \\ H(z + \Delta z) \end{pmatrix}$$

$$= \begin{pmatrix} \cos(k_0 n \Delta z) & -i/n \sin(k_0 n \Delta z) \\ -in \sin(k_0 n \Delta z) & \cos(k_0 n \Delta z) \end{pmatrix} \begin{pmatrix} E(z) \\ H(z) \end{pmatrix},$$

$$(2)$$

where $H(z,t) = -\frac{i}{\omega}\frac{\partial E(z,t)}{\partial z}$.

The boundary condition is that of a traveling wave in the substrate. The wave vectors of the plane waves are taken as complex numbers. This is a consequence of defining the refraction index as a complex quantity:

$$n_j = \eta_j + i\kappa_j, \quad (j = 1, 2),$$

$$(3)$$

in order to allow for absorption effects to be included directly in our calculation. A simplification is often used in which an effective refraction index, defined by

$$\langle n \rangle = \left[\left(n_1^2 d_1 + n_2^2 d_2 \right) / d \right]^{\frac{1}{2}},$$

$$(4)$$

is assumed for both constituent materials.[1] Here, d_1 and d_2 denote the thickness of the layers, and d the SL period. Let us note that an identical refractive index for the two media is equivalent to the absence of reflections of electromagnetic waves at the interfaces. This assumption was shown to be valid in absence of any absorption effect by the authors of Refs. 6 and 8 except for the Bragg conditions for the reflection of light, that corresponds to $q/q_{mz} = 2, 4, 6, \ldots$, where $q_{mz} = \pi/d$ is the minizone boundary wave vector.

In order to compare the results of the calculation using the transfer-matrix method with this approximation, we plot in Fig. 1 the electric field amplitudes vs the penetration depth, D. The upper curves in this figure show the comparison for a superlattice of $Si/Ge_{0.44}Si_{0.56}$ with twenty repetitions of $d_1 = 26.5$ nm and $d_2 = 5.0$ nm. It can be seen in this figure that the transfer-matrix method
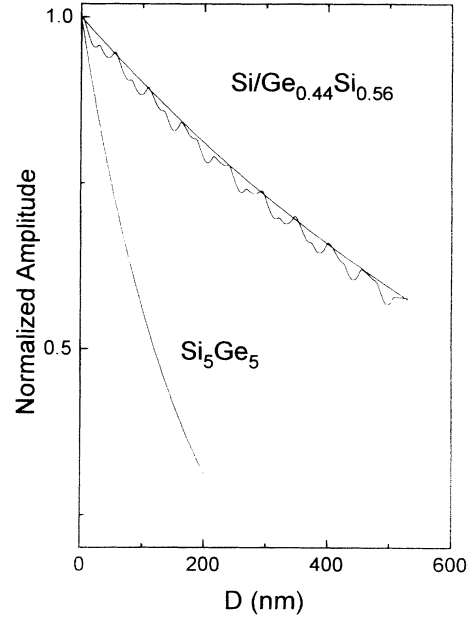

FIG. 1. Normalized electric field amplitudes for a $Si/Ge_{0.44}Si_{0.56}$ superlattice with $N = 20$ periods (upper curves), obtained with the transfer-matrix method (oscillatory trace) and using the effective refraction index (exponential decay). The lowest trace shows the last calculation for the much absorbing Ge_5Si_5 superlattice with $N = 145$.

results yield a profile of small oscillations which does not differ appreciably from the exponential decay curve. Hence the approximation of effective refraction index introduces negligible differences compared with the results of applying (2). Besides, it is much simpler than (2) in the calculation of the scattering intensity.

However, it is crucial in the latter case to take into proper account the absorption in Eq. (1) through the imaginary part of the refraction index. The effect of the absorption is illustrated in Fig. 1, lower curve. Here, a Si_5Ge_5 superlattice with 145 periods was chosen as an example. The choice was based on the fact that the extinction coefficient is about five times bigger in this sample than in the $Si/Ge_{0.44}Si_{0.56}$ superlattice. Besides, this is the superlattice used further on in this description to compare final results with experiment. It is worthwhile mentioning that the presence of absorption allows for the linewidth of the Raman peaks to be properly accounted for.

III. ELASTIC WAVES PROPAGATION

The calculation by a transfer-matrix method of the vibrational modes is very similar to the one described above for the electromagnetic fields. In fact, replacing E and H, which propagate without discontinuity along the layers, with the phonon amplitudes $u(z)$ and the stresses $C_j du/dz$, we can write the transfer matrix for elastic waves:

$$\begin{pmatrix} u(z + \Delta z) \\ C_j(\frac{du}{dz})|_{z+\Delta z} \end{pmatrix}$$

$$= \begin{pmatrix} \cos(k_j\Delta z) & \sin(k_j\Delta z)/(C_j k_j) \\ -C_j k_j \sin(k_j\Delta z) & \cos(k_j\Delta z) \end{pmatrix}$$

$$\times \begin{pmatrix} u(z) \\ C_j(\frac{du}{dz})|_z \end{pmatrix}, \qquad (5)$$

where $k_j = \frac{\omega}{v_{jL}}$ is the wave vector of the longitudinal mode of frequency ω in the medium with sound velocity v_{jL}, $j = 1, 2$.

Here we take stress free boundary conditions at the air-superlattice (or air-capping layer) interface, which produce stationary wave solutions. The amplitudes of the modes are normalized to the amplitude in the substrate. This is equivalent to assuming the substrate infinite, because we consider that the density of states of the SL is a small perturbation of the total density of states of SL plus substrate. The normalized mode patterns $u(p, z)$ and the associated strains $\epsilon_{zz} = \frac{\partial u_z(p,z)}{\partial z}$ are calculated as functions of the frequency with as small a step as necessary. The acousto-optic parameter $P(z)$, whose main effect is to determine the relative intensities of the modes in the spectra, has yet to be discussed. All other quantities appearing in (1) can be calculated if the parameters of the materials, like refraction indexes, layer thickness, elastic constants, and sound velocities are known. These quantities are known with some uncertainty and we are faced with the inverse problem: to determine the values of these quantities from the Raman spectra. Actually, the parameters of the materials can be determined independently since they are related to different aspects of the line shapes of the spectra. To pursue this idea, it is necessary to analyze in some detail the role of the three terms appearing in the integral of (1). The integration in (1) is taken as a sum in a finite size SL with the effective range determined by the decay in electric field due to the absorption of light. The contribution of the different vibrational modes will be determined by their amplitudes in the scattering volume. This can be taken into account by considering a density of state projected on a definite range of z near to the surface, the projected density of states (PDOS). The PDOS can be measured by the mean square amplitude of the modes in the region of interest. We studied the problem in detail for some systems, and found that the PDOS is strongly sensitive to the structure of the SL. To illustrate this point we selected three examples: a thin layer Ge_5Si_5 SL with $N = 145$, and two thick-layer $Si/Ge_{0.44}Si_{0.56}$ superlattices of identical structures, except for the number of periods, which are $N = 20$ and 200, respectively. Figure 2(a) [Fig. 2(e)] shows the dispersion relation for the thin layer SL (thick layer SL). The dispersion curves for the thick layer SL's consist of several folded branches. In contrast, the thin layer SL dispersion curve in the same frequency range is a single branch since the first folding is expected to occur at about 70 cm^{-1}. The traces 2(b), 2(c), and 2(d) are the PDOS, projected on the SL, corresponding to the Ge_5Si_5 superlattice and to the $Si/Ge_{0.44}Si_{0.56}$ superlattice with

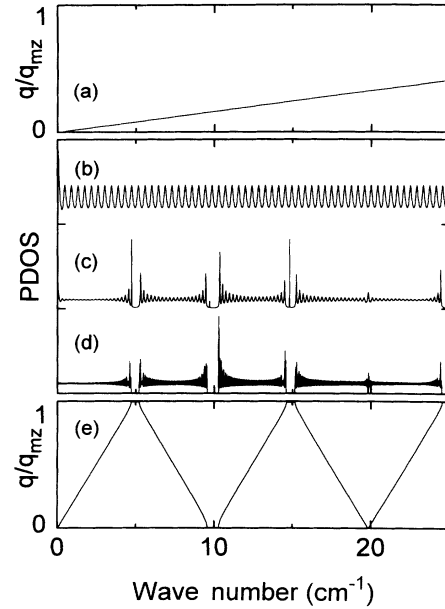FIG. 2. Dispersion relation curves for (a) a Ge_5Si_5 superlattice with $N \to \infty$ periods; (e) a $Si/Ge_{0.44}Si_{0.56}$ superlattice with $N \to \infty$; projected density of states for (b) same as (a) but $N = 145$; (c) same as (e) but $N = 20$ periods; and (d) same as (e) but for $N = 200$ periods.

$N = 20$ and 200 periods, respectively. The plot 2(b) is a highly structured function of ω, showing several small oscillations which are related to the number of periods of the SL. Actually, due to the finite-size effects, there are 145 oscillations per branch in the dispersion relation. In the intermediate curve, Fig. 2(c), the number of small oscillations per branch is 20. Finally, at the lower curve, Fig. 2(d), corresponding to $N = 200$, the 200 oscillations per branch merge into a quasicontinuum PDOS, very similar to the one that can be calculated for an ideal infinite SL when the well known Rytov's relation[13] is used. It is worthwhile mentioning that the latter curve lacks structures in the ranges of frequency corresponding to the gaps in the dispersion curve of Fig. 2(e). This behavior contrasts with the finite-size ($N = 20$) SL of Fig. 2(c), where several peaks are seen inside the gap region. These features, also present in the plots of transmission coefficient, were interpreted in terms of resonance phonon modes arising from the interaction between the continuum of phonon states from the substrate and the modes of the SL.[11] In a following paper we report on the first observation of such modes, for several Si/Ge_xSi_{1-x} superlattices with varying structures.[14] As we shall see soon in the example of the next section, the use of the PDOS, which actually does not enter the calculation of the scattering, is important because it gives the energy position of the structures in the spectra. In this way, the structural and dynamical parameters of the material can be determined independently from the optical and acousto-optical ones.

IV. COMPARISON WITH EXPERIMENT

As a test for our method of calculation we use a thin layer superlattice grown on a (001) Si substrate by alternating 5 monolayers of Ge and 5 of Si, (Ge_5Si_5). The sample was prepared to produce a symmetrically strained superlattice.[15] The total thickness was 215 nm and $N=145$. Since $qd \ll 1$, the phase of the exciting electric field is almost constant over a Ge_5Si_5 layer and a single effective value of the acousto-optic coefficient for each layer can be considered. Furthermore, one can try to assume $P(z)$=const in (1) along the 145 Ge_5Si_5 layers, by neglecting long range effects and assuming that P depends only on the local properties of the material. Figure 3 displays the experimental and calculated spectra. The experimental spectra clearly show the Brillouin peak with a superimposed modulation. These structures are due to the finite size of the SL and reflect the corresponding modulation of the PDOS shown in the inset of Fig. 3. The separation is constant for a given structure of the superlattice and depends on the vibrational dynamics, so that it is the same for the two excitations. Since the energy separation between two successive peaks in the PDOS is $\Delta\omega = (v\pi)/(Nd)$, the mean velocity of sound is obtained from the measurement of the separation of the peaks in the spectra, $\Delta\omega$=0.46 cm^{-1}. The resulting mean velocity value, $v = 5.6 \ 10^5$ cm/s, was used as input in our computational procedure. The numerical values for d_1 and d_2 were 6.7 nm and 7.2 nm, respectively. They were determined by combining information on total thickness (215 nm) and the number of layers. The elastic constants C_j present in the transfer matrices can be deduced from the velocity of sound and from the density. Since v was determined experimentally we used

for the densities the nominal figures for pure Si and pure Ge, i.e., 2.33 g/cm^3 and 5.36 g/cm^3, respectively.

The profiles of the spectra can be fitted with two adjustable parameters, the real and imaginary parts of the refraction index. These quantities play two different roles: the real part determines the center of the Brillouin peak, whereas the imaginary part determines the overall linewidth. The fitting yielded $\langle n \rangle = 6.35 + 0.477i$ for λ=514.5 nm and $\langle n \rangle = 6.45 + 0.67i$ for λ=496.5 nm. While the imaginary parts fits very well the extrapolated values from published data for bulk $Ge_{0.5}Si_{0.5}$ compounds,[16] the real parts are higher than in the corresponding bulk alloy. At first, one might have expected the Ge_5Si_5 SL parameters to be close to those of the bulk $Ge_{0.5}Si_{0.5}$ compound. This is not the case of the strain-symmetrized SL of this work. The crystals in the few constituent monolayers are strained in such a way as to modify significantly the electronic band structure.[17] The electronic band structure and the dielectric response, in turns, have been found to be very sensitive to n and m in short-period Ge_nSi_m strained-layer SL.[17] Considering that we are probing at 2.4–2.5 eV, where the onset of the strong absorption occurs, we expect a maximum for the real part of the dielectric constant at approximately this energy and a value of the index of refraction between the maxima observed for bulk Si and Ge. This is precisely what happens with our data. For instance, we obtained $\eta \approx 6.4$, whereas $\eta_{max}^{Si} = 7.0$ and $\eta_{max}^{Ge} = 5.5$.

The application of the computational method to SL with small values of d is very simple since it does not need the knowledge of the $P(z)$ profile. In order to have information on the acousto-optic properties of the materials one has to study SL with thicker layers. Actually, for $qd \approx 1$ the $P(z)$ profile becomes of fundamental importance. The problem is going to be discussed in a following paper.[14]

V. CONCLUSION

We have described a numerical calculation of Raman scattering by acoustic phonons by using a transfer-matrix method to account for the elastic properties. This method has relevant practical advantages compared with the method proposed by He *et al.*[6] First of all, our calculation can be performed for any given sequence of layers, including the capping layer and the substrate, and not only for infinite SL's, as in the case of Ref. 6. This is of great importance since real SL's consist, in general, of 10 to 100 periods of alternating pure and alloy layers, grown on pure substrates. In such a system the actual vibrational dynamics can greatly differ from the one deduced for an infinite SL. In particular, the phonons of the substrate act like a thermal bath and phonons with energies within the minigaps of the SL can penetrate into many layers. This is the reason why an appreciable density of vibrational states in the SL can be found also at the minigap energies at variance with the prediction of the model of an infinite SL. On the other hand, the use of an infinite substrate, coupled to the finite SL, allows for the calculation of a continuous density of states. Conse-
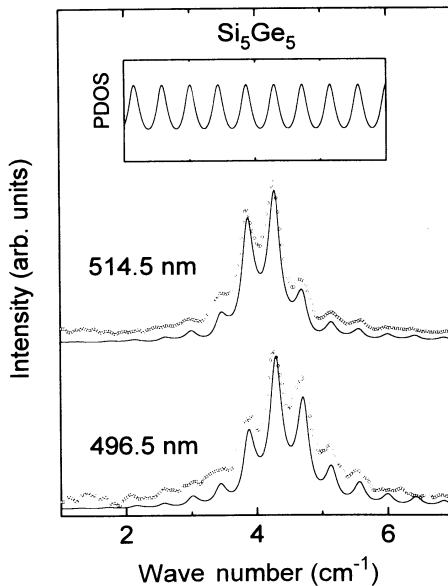

FIG. 3. Calculated (solid line) and experimental Brillouin spectra (circles) for a Ge_5Si_5 superlattice with $N = 145$ periods. The inset displays the PDOS in the SL in the same frequency range.

quently, the spectrum can be calculated with a frequency spacing as small as necessary to reproduce its finest structures including the very sharp gap modes. This presents important advantages with respect to the linear chain model,[18] where a finite substrate is taken into account, failing in some cases to give the details of the fine structure and introducing instead spurious effects. Comparison with experiment displays quantitative agreement, including detailed features like small oscillations modulating the Brillouin line. In view of the perfect agreement between calculated and measured spectra we propose this computational method of modeling a SL as a tool in the characterization of real systems. The calculation can be extended to any multilayered system by inputting appropriate structural parameters. The fit of our results to experiment leads to a method for the determination of physical characteristics of the microstructure.

ACKNOWLEDGMENTS

* On leave from Dipartimento di Fisica, Università degli Studi di Trento, Trento, Italy.

[1] P.X. Zhang, D.J. Lockwood, H.J. Labbé, and J.-M. Baribeau, Phys. Rev. B 46, 9881 (1992).

[2] V. Lemos, O. Pilla, M. Montagna, P. Benassi, A. Fontana, C.F. de Souza, and W. Carvalho, Jr., Braz. J. Phys. 24, 214 (1994).

[3] D.J. Lockwood, M.W.C. Dharma-wardana, J.-M. Baribeau, and D.C. Houghton, Phys. Rev. B 35, 2243 (1987), and references therein.

[4] M.W.C. Dharma-wardana, P.X. Zhang, and D.J. Lockwood, Phys. Rev. B 48, 11 960 (1993).

[5] C. Colvard, T.A. Gant, M.V. Klein, R. Merlin, R. Fisher, H. Morkoc, and A.C. Gossard, Phys. Rev. B 31, 2080 (1985).

[6] J. He, B. Djafari-Rouhani, and J. Sapriel, Phys. Rev. B 37, 4086 (1988).

[7] B. Jusserand, D. Paquet, F. Mollot, F. Alexandre, and G. Le Roux, Phys. Rev. B 35, 2808 (1987).

[8] J. Sapriel, J. He, B. Djafari-Rouhani, R. Azoulay, and F. Mollot, Phys. Rev. B 37, 4099 (1988).

[9] G.C. Aers, M.W.C. Dharma-wardana, G.P. Schwartz, and

J. Bevk, Phys. Rev. B 39, 1092 (1989); M.W.C. Dharma-wardana, G.C. Aers, D.J. Lockwood, and J.-M. Baribeau, ibid. 41, 5319 (1990).

[10] D.J. Lockwood, M.W.C. Dharma-wardana, G.C. Aers, and J.-M. Baribeau, Appl. Phys. Lett. 52, 2040 (1988).

[11] S. Mizuno and S. Tamura, Phys. Rev. B 45, 13 423 (1992); 45, 734 (1992); S. Tamura, ibid. 43, 12 646 (1991).

[12] J. He, J. Sapriel, and R. Azoulay, Phys. Rev. B 40, 1121 (1989).

[13] S.M. Rytov, Akust. Zh. 2, 71 (1956) [Sov. Phys. Acoust. 2, 68 (1956)].

[14] V. Lemos, O. Pilla, M. Montagna, and C.F. de Souza, International J. Superlatt. Microstruct. (to be published).

[15] E. Kasper, H. Kibbel, H. Jorke, H. Brugger, E. Friess, and G. Abstreiter, Phys. Rev. B 38, 3599 (1988).

[16] J. Humliček, M. Garriga, M.I. Alonso, and M. Cardona, J. Appl. Phys. 65, 2827 (1989).

[17] U. Schmid, N.E. Christensen, M. Alouani, and M. Cardona, Phys. Rev. B 43, 14 597 (1991).

[18] M.W.C. Dharma-wardana, P.X. Zhang, and D.J. Lockwood, Phys. Rev. B 48, 11 960 (1993).